Exhuming the Remains of the Inactive Mountain-Front Pirate Fault, Santa Catalina Mountains, Southeastern Arizona

Dwight T. Hoxie
U.S. Geological Survey (Retired)

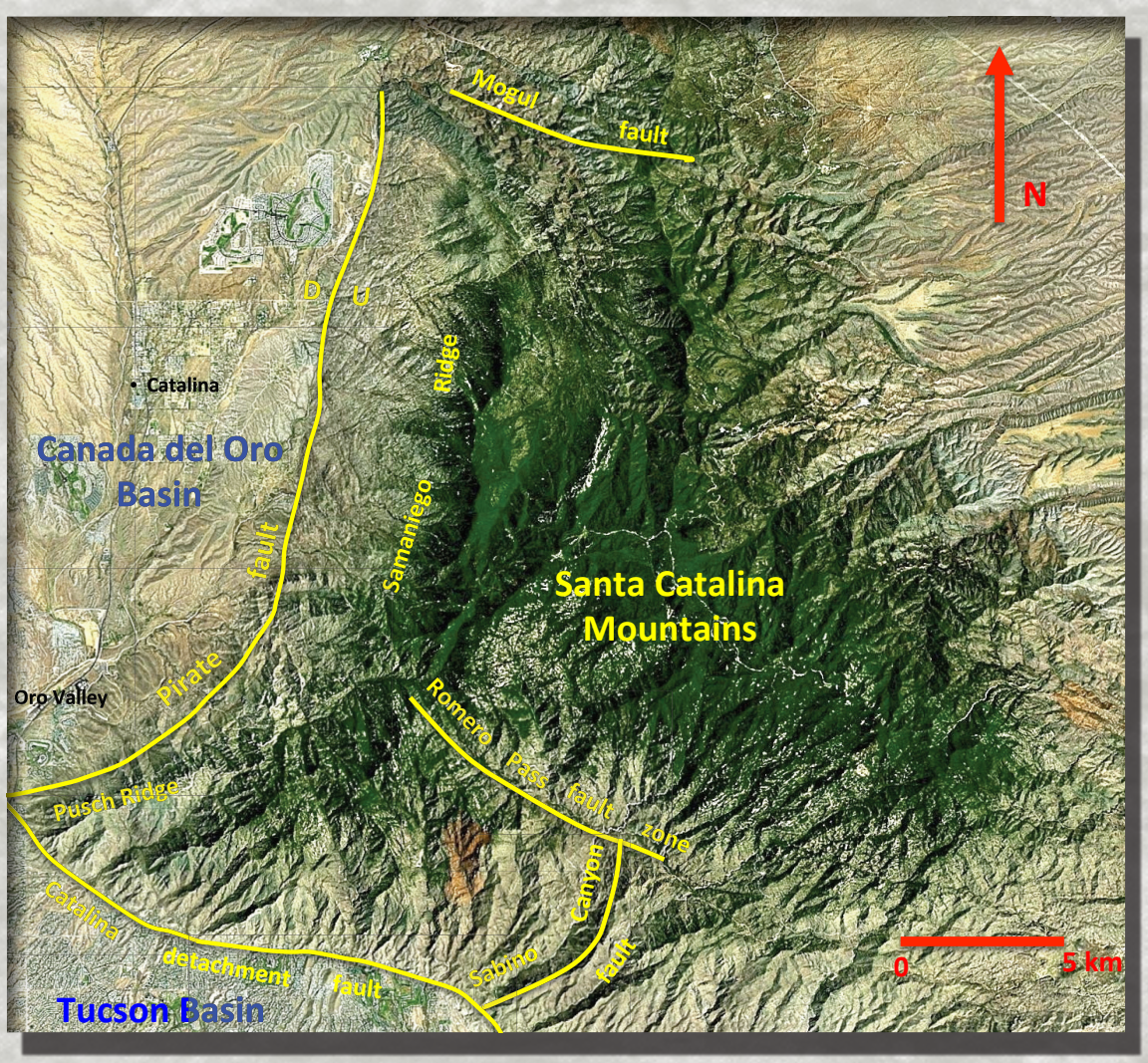

Santa Catalina Mountains, Tucson, Arizona

CONTRIBUTED REPORT CR-12-F

November 2012

Arizona Geological Survey

www.azgs.az.gov | repository.azgs.az.gov

Arizona Geological Survey

M. Lee Allison, State Geologist and Director

Manuscript approved for publication in November 2012
Printed by the Arizona Geological Survey
All rights reserved

For an electronic copy of this publication: www.repository.azgs.az.gov
Printed copies are on sale at the Arizona Experience Store
416 W. Congress, Tucson, AZ 85701 (520.770.3500)

For information on the mission, objectives or geologic products of the Arizona Geological Survey visit www.azgs.az.gov.

This publication was prepared by an agency of the State of Arizona. The State of Arizona, or any agency thereof, or any of their employees, makes no warranty, expressed or implied, or assumes any legal liability or responsibility for the accuracy, completeness, or usefulness of any information, apparatus, product, or process disclosed in this report. Any use of trade, product, or firm names in this publication is for descriptive purposes only and does not imply endorsement by the State of Arizona.

Recommended Citation: Hoxie, D.T., Exhuming the Remains of the Inactive Mountain-Front Pirate Fault, Santa Catalina Mountains, Southeastern Arizona. Arizona Geological Survey Contributed Report CR-12-F, 18 p.

Arizona Geological Survey Contributed Report CR-12-F

Exhuming the Remains of the Inactive Mountain-Front Pirate Fault, Santa Catalina Mountains, Southeastern Arizona

November 2012

Dwight T. Hoxie
U.S. Geological Survey (Retired)

Arizona Geological Survey Contributed Report Series

The Contributed Report Series provides non-AZGS authors with a forum for publishing documents concerning Arizona geology. While review comments may have been incorporated, this document does not necessarily conform to AZGS technical, editorial, or policy standards.

The Arizona Geological Survey issues no warranty, expressed or implied, regarding the suitability of this product for a particular use. Moreover, the Arizona Geological Survey shall not be liable under any circumstances for any direct, indirect, special, incidental, or consequential damages with respect to claims by users of this product.

The author(s) is solely responsible for the data and ideas expressed herein.

ABSTRACT

The ~25 km accessible trace of the north-south trending, west-side down, normal, mountain-front Pirate fault has been mapped to locate and describe those erosionally exhumed remnants of the fault that together provide a basis for structural reconstruction of this nominally Basin-Range tectonic feature. The fault forms the western boundary of the Santa Catalina Mountains in southeastern Arizona, where it separates the uplifted Santa Catalina structural block on the east from the down-dropped, alluvial Cañada del Oro basin on the west. Vertical displacement on the fault is estimated to be ~4 km, accumulated over a ~6 my active duration from ~12 to ~6 Ma. Following cessation of active uplift, the fault was buried under detritus eroded from the uplifted Santa Catalina block and, currently, is being exhumed by the downcutting Cañada del Oro and its tributaries. This field examination reveals the fault to have left a sparse but diverse collection of remains implying a varied history of fault development and evolution.

INTRODUCTION

For many who reside in the Tucson, Arizona, metropolitan area a singular attraction is the conspicuous escarpment that forms the west face of the Santa Catalina Mountains. The Santa Catalina Mountains constitute a structural block that rises abruptly from a valley-floor altitude of ~900 m in the Tucson-basin to a summit altitude of ~2800 m to the north and east of the city. The escarpment that delineates the west face of the mountain block extends northward from the sheer cliffs of Pusch Ridge in the southwest for ~30 km along a pediment excavated in granitic rocks below the north-trending Samaniego Ridge (Fig. 1). While the escarpment is a conspicuous topographic feature, its origin as the remnant of an eroded fault-line scarp along the now inactive Pirate fault is not well known. The Pirate fault is a Basin-Range mountain-front normal fault that, during its active lifetime 12-6 Ma (Dickinson, 1994), resulted in ~4 km of vertical displacement in which the Cañada del Oro basin on the west subsided to a depth of ~2.5 km below present-day land surface while the Santa Catalina mountain block rose on the east to the present-day ~2.3 km altitude of Samaniego Ridge (Dickinson, 1994; Davis, et al., 2004; Fig. 1). Of the fault itself, there remains only a remnant fault trace together with intermittent exposures of fault rocks and features. The accessible trace of the fault extends north-south for ~25 km from a northern terminus beneath basin fill about 11 km northeast of the town of Catalina to a southern terminus beneath basin fill about 6 km southeast of the Oro Valley town center (Fig. 1).

This paper reports the results of a field investigation to map the total accessible extent of the Pirate fault specifically to locate and describe those remnant features of the fault on which construction of a model of fault formation and development could be based. The study reveals the fault to be an aggregate of disparate features and characteristics superimposed on a fault trace that, in the main, can be interpreted in terms of a relatively simple conceptual model of fault genesis. Most of the observed disparities are matters of detail that can be accommodated within the overall conceptual framework but some present problems of interpretation that remain unresolved.

A total of twenty sites of exposed fault rocks and/or fault-related features were mapped along the accessible trace of the Pirate fault during this study and are shown in Figs. 2A-E in which filled triangles denote sites of exposed fault-core rocks and filled rectangles denote mafic dikes that appear to delineate the fault along about one-third of its trace. The sites are color coded according to the host rock in which they are located according to the scheme indicated in Table 2 and are labeled by their abbreviated site names, e.g., DHG = Dead Hawk Gulch. Ten sites were selected for description in this report (Table 1), which gives the site name (as informally defined for use in this study), UTM coordinates (in accordance with the convention below), and a summary description of the diagnostic fault-related characteristics or features exposed at the site. The abbreviated site names are used throughout the text when referencing the individual sites listed in Table 1. Site locations are given by Zone 12 Universal Transverse Mercator (UTM) coordinates (North American Datum of 1983) using the convention "(xxxxxxx yyyyyyy)," where "xxxxxxx" = easting and "yyyyyyy" = northing. Base maps for Figs. 2A-E are taken from the United States Geological Survey "Oro Valley," "Mount Lemmon," "Oracle," and "Tucson North" 1:24,000 topographic maps. For simplicity, the fault is depicted in Figs. 2A-E as a continuous line drawn between its projected northern and southern endpoints.

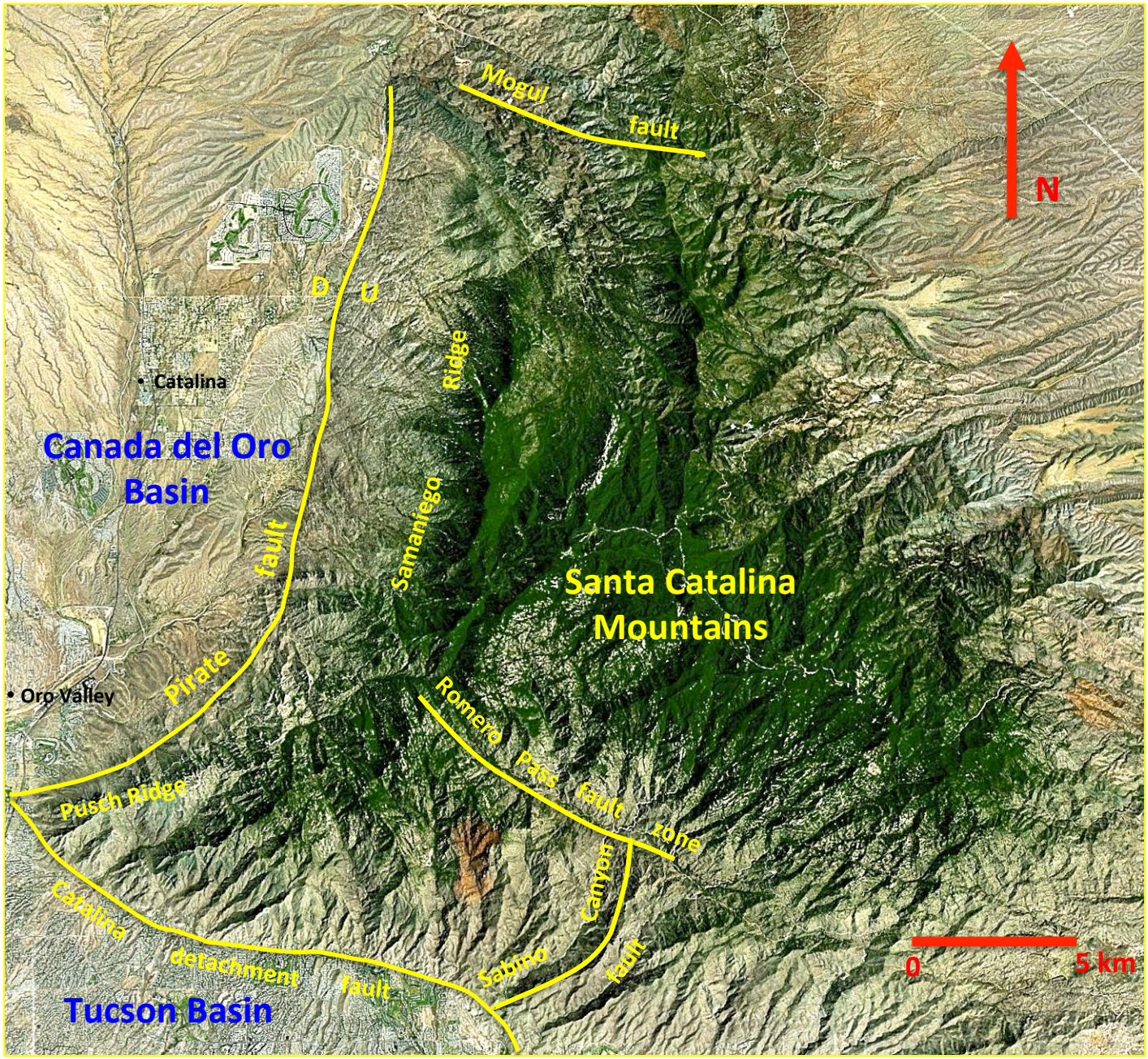

Figure 1. Satellite image of the Santa Catalina Mountains and adjacent Tucson and Cañada del Oro basins showing locations of Samaniego Ridge, Pusch Ridge, and Catalina and Oro Valley town sites and approximate traces of the Pirate fault, Sabino Canyon fault, Mogul fault, Catalina detachment fault, and Romero Pass fault zone.

BACKGROUND

The Santa Catalina Mountains and adjoining Tucson basin to the south and Cañada del Oro basin to the west (Fig. 1) lie within the Mexican Highland subprovince of the Basin and Range physiographic province (Fenneman, 1931). The Basin and Range province of the southwestern U.S. is characterized by fault-bounded, generally north-south trending mountain ranges separated by deep intermontane alluvial basins that formed during the extensional Mid- to Late-Miocene Basin-Range tectonic event (Eaton, 1982). The normal, down-to-the-west Pirate fault is construed to be a Basin-Range bounding fault (Dickinson, 1994) separating the bedrock core of the Santa Catalina Mountains on the east from the alluvial Cañada del Oro basin on the west (Fig. 1). Uplift of the Santa Catalina Mountains footwall combined with down-dropping of the hanging wall during the Basin-Range tectonic event led to formation of the Cañada del Oro basin, which subsequently was filled by debris eroded from the uplifted Santa Catalina block on the east and from lower-altitude mountain highlands on the west. Deposition of basin-fill material in the Cañada del Oro basin culminated in Pleistocene time (1-2 Ma) following cessation of active uplift on the Pirate fault. Alluvium deposited during this latter time forms the high-stand Cordones surface of coalescent

Table 1. Site name and abbreviated designator, UTM location, and summary description of principal fault-related characteristics of field sites discussed in text.

Name	Location Easting | Northing	Description
XP Wash (XPW)	0514450 3602387	Hematite-free fault core and damage zone in Xp host rock.
Dead Hawk Gulch (DHG)	0514332 3601844	Hematite-rich fault surface, core, and damage zone in Tgc host rock.
Golder Dam (GD)	0514011 3600454	Exposed hematite-rich fault surface and core with mafic dike intrusion inTgc host rock.
Mafic Dike Set (MFD)	0512527 3595544	Representative site of mafic dikes intruding Tgcg breccia and aligned parallel to fault trace in Tgc host rock.
Romero-Cargadero Fault-Rock Zone (RCX)	0510313 3588634	Hematite-free, leucogranite brecciated/fractured damage zone abutting Tgw host rock.
Breccia Hill Complex (BHC)	0510085 3587990	Hematite-free, indurated fault-breccia outcrops overlying brecciated/fractured damage zone abutting Tgw host rock.
Pirate Knob (PK)	0508609 3586171	Hematite-rich fault surface and vesicular fault-core cataclasite in Tgw host rock.
Alamo Canyon (ALC)	0508315 3585856	Hematite-rich fault surface, core, and damage zone in Kga host rock with anomalous hematite-free leucogranite block on hanging wall.
Pusch Ridge Wilderness (PWR)	0507604 3585292	Hematite-rich fault surface, core, and damage zone in Kga host rock.
Linda Vista Trail (LVT)	0504309 3582133	Hematite-rich fault core rocks in Kga host rock.

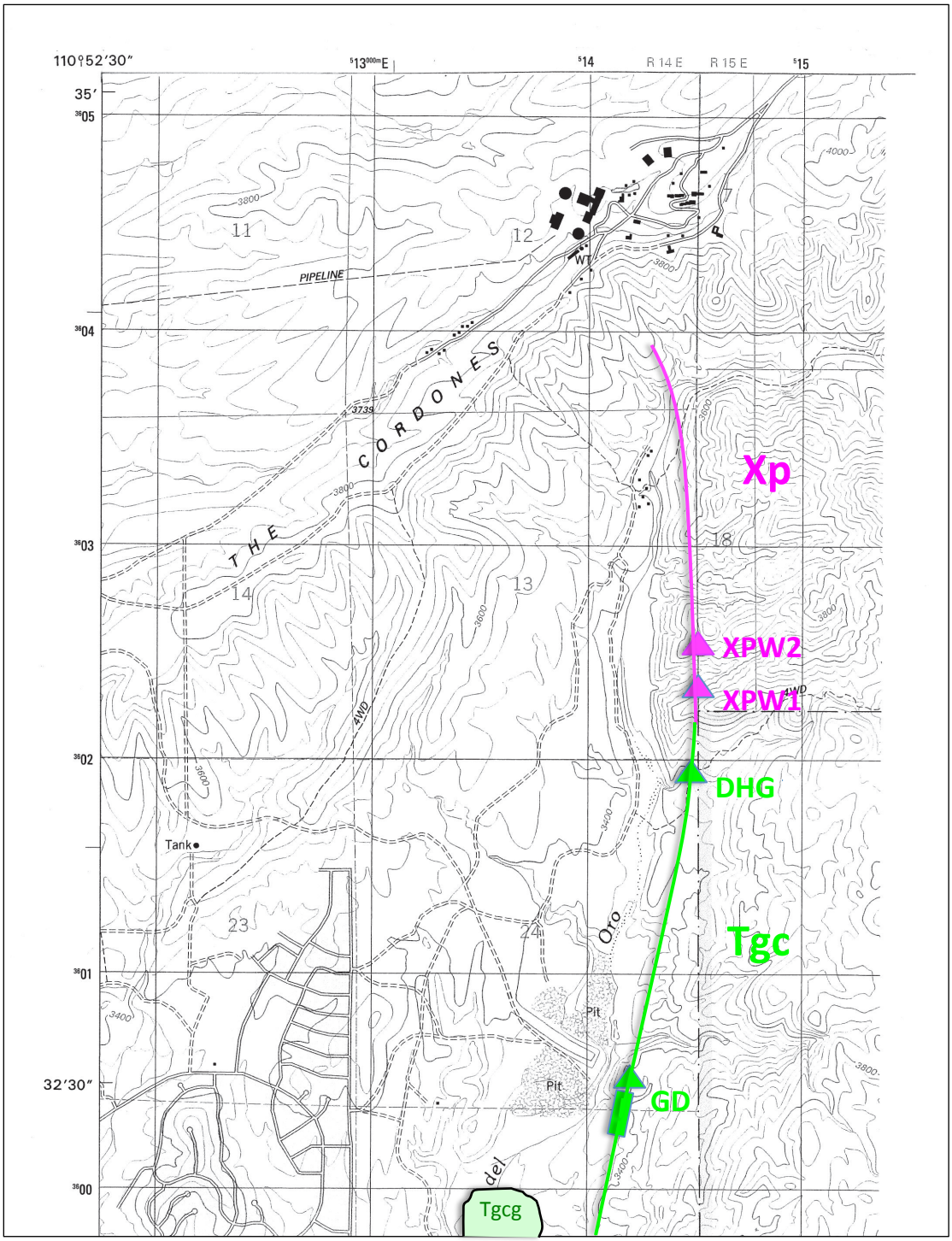

Figures 2A-E. Maps of the trace of the Pirate fault from north to south showing sites (Table 1) of exposed fault core rocks (colored triangles), fault-aligned mafic dikes (colored rectangles), and projected trace (dashed red line) of possible relict Romero Pass fault zone (Fig. 2D).

Figures 2B-E follow on the next page.

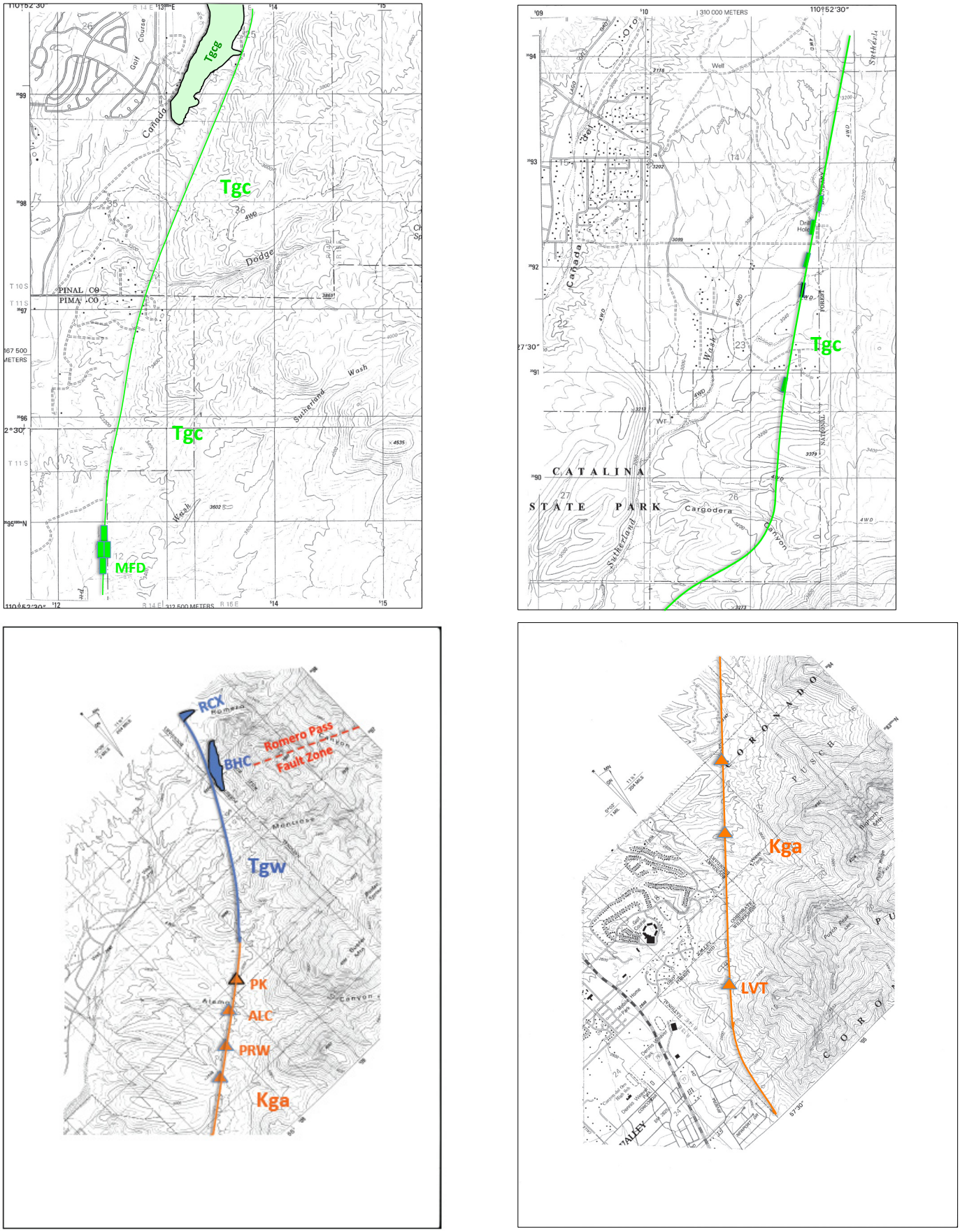

Figures 2B-E. Maps of the trace of the Pirate fault from north to south showing sites (Table 1) of exposed fault core rocks (colored triangles), fault-aligned mafic dikes (colored rectangles), and projected trace (dashed red line) of possible relict Romero Pass fault zone (Fig. 2D).

alluvial fans composed mostly of detritus eroded from the Santa Catalina Mountains (Menges and McFadden, 1981). Subsequent removal of basin-fill material by the downcutting Cañada del Oro and its tributaries produced the ridge and ravine topography of the present-day Cañada del Oro basin and, additionally, exposed the formerly buried trace of the Pirate fault.

Timing of the Basin-Range event with specific regard to the active tectonic life of the Pirate fault is poorly constrained. Study of two basins in southeastern Arizona (Menges and McFadden, 1981), the Sonoita Creek basin ~ 80 km southeast of Tucson and the Cañada del Oro basin adjacent to the Santa Catalina Mountains (Fig. 1), however, suggests that Basin-Range tectonism largely ceased in southeastern Arizona in the interval between 6 and 3-2 Ma. Principal activity on the Pirate fault is considered to have occurred during Mid- to Late-Miocene time (12-6 Ma) (Dickinson, 1994) followed by active pedimentation to produce the present-day 2-4 km wide pediment along the western face of the Santa

Table 2. Geologic units cited	
Qal	**Quaternary alluvium (undifferentiated)** Refers principally to weakly cohesive gravels capping dissected, coalescent Pleistocene alluvial fans along the west face of the uplifted Santa Catalina structural block. Composed mostly of granitic pebbles, cobbles, and boulders with variable admixture of sand and clay to form much of the hanging-wall block on the west side of the north-south trending Pirate fault. Manifest as the high-stand Cordones surface of Menges and McFadden (1981).
Tgcg	**Catalina granite grus (Late Miocene)** Variably cohesive, stratified, poorly graded and sorted arkosic sand and grus with pebble-to-cobble-sized Tgc inclusions that forms the hanging-wall block of the Pirate fault in Tgc host rock and, additionally, locally forms steep valley sides and indurated "bedrock" floor of the north-south draining Cañada del Oro.
Tgc	**Catalina granite (Oligocene ~26 Ma)** Porphyritic biotite granite pluton with conspicuous orthoclase phenocrysts up to ~ 8 cm in an assemblage of otherwise subequal quartz, K feldspar, and plagioclase. Contains abundant mafic xenoliths ranging from centimeters to meters in extent and numerous aplite dikes (Force, 1997; Spencer and Pearthree, 2004).
Tgw	**Wilderness granite (Eocene ~47 Ma)** Lowermost of leucocratic granite sills intruding Proterozoic Pinal schist (Xp) and Cretaceous biotite granite of Alamo Canyon (Kga). Medium-to-coarse-grained equigranular quartz, orthoclase, and plagioclase with approximately subequal muscovite and biotite with 1-2 percent euhedral garnet (Force, 1997, Table 9) and containing numerous aplite and pegmatite dikes (Force, 1997).
Kga	**Biotite granite of Alamo Canyon (Cretaceous ~70 Ma)** Foliated, fine-to-medium-grained, equigranular, quartz/feldspar biotite granite widely intruded by 2 to 200 cm-thick dikes and sills of Tgw leucogranite and pegmatite (Spencer and Pearthree, 2004).
Xp	**Pinal schist (Proterozoic ~1.65 Ga)** At the XPW1 and XPW2 sites (Fig. 2A), gray to tan, laminated greywacke and shale with included quartz stringers and pods.

Catalina Mountains (Menges and McFadden, 1981).

PIRATE FAULT MORPHOLOGY

The accessible trace of the Pirate fault extends southward ~25 km (Fig. 1) from its northern terminus beneath basin-fill alluvium underlying the Cordones surface (Fig. 2A) to its southern disappearance beneath the alluvial floor of the Tucson basin (Fig. 2E). Over this distance the fault transects four bedrock units (Dickinson, 1994; Spencer and Pearthree, 2004) consisting, from north to south, of Proterozoic Pinal schist (Xp), early Miocene Catalina granite (Tgc), Eocene Wilderness granite (Tgw), and Cretaceous biotite granite of Alamo Canyon (Kga). Summary descriptions of these units are given in Table 2 together with description of the informally named "Catalina granite grus" (Tgcg), which was defined and mapped as part of the present study. The fault trace and field sites shown in Figs. 2A-E are color coded by host-rock geologic unit according to the following scheme as defined in Table 2: Xp (magenta), Tgc (green), Tgw (blue) Kga (orange), and Tgcg (green).

A number of studies have investigated various aspects of the fault beginning with Wallace (1954) who bestowed the name "Pirate fault" to this structural feature. Dickinson (1994) mapped the complete trace of the fault at a scale of 1:24,000 using the contact between basin-fill alluvium on the west and footwall bedrock on the east to delineate the fault trace. Spencer and Pearthree (2004) show and describe in some detail features of the fault they identified in their mapping of the Oro Valley 1:24,000 Quadrangle. Davis et al. (1994, 1998, 2004) provide detailed description of a cross-section through the fault from fault surface to footwall Tgc host rock at informally named Dead Hawk Gulch (DHG) (Fig. 2A).

Compositional continuity of hanging-wall detritus with footwall host rock across the Pirate fault indicates that movement on the fault was predominantly dip-slip with little or no strike-slip component (Dickinson, 1994). Measurement of fault-surface attitude indicates the fault to be a planar feature with a consistent dip of 50-55° to the west along the entire exposed trace of the fault (Dickinson, 1994). Gravity modeling of the Cañada del Oro basin (Davis, et al., 2004) suggests the basin to be a half-graben with a depth of ~2.5 km below land surface along a fault that becomes increasingly listric with depth. Taking the crest of Samaniego Ridge (Fig. 1) at an altitude of ~2300 m to represent the eroded remnant of the uplifted Santa Catalina structural block (Dickinson, 1994) together with a valley floor altitude of ~900 m and basin depth of 2.5 km (Davis, et al., 2004) implies a vertical displacement on the Pirate fault of ~4 km.

The accessible trace of the Pirate fault terminates to the north at about (0514200 3603900) (Fig. 2A) where it disappears beneath alluvium of the Cordones surface and to the south at about (0503600 3580600) (Fig. 2E) where it disappears beneath valley-fill alluvium of the Tucson basin. Beyond these termination points, however, the fault nominally intersects two pre-existing structural features that likely influenced development of the fault. To the north, inferred extension to the west of the southeast-to-northwest trending Mogul fault (Fig. 1) (Dickinson, 1992; Force, 1997) and projected northward continuation of the Pirate fault intersect near (0515003 3605912), ~200 m northeast of the northern terminus of the fault shown in Fig. 2A. This location is that of a decorative-stone quarry whose source rock is highly fractured, deformed, and altered bedrock (possibly Xp?) that may be evidence of the projected fault intersection. To the south, the Pirate fault intersects the east-west trending, low-angle Catalina detachment fault (Fig. 1) (Dickinson, 1994, 1999), but, because of alluvial cover, the intersection of the two faults is inaccessible to direct examination. Nevertheless, the presence of the Mogul fault to the north and the Catalina detachment fault to the south prior to emplacement of the Pirate fault may have influenced its development, perhaps serving to fix its north and south endpoints, respectively.

A CONCEPTUAL MODEL OF PIRATE FAULT GENESIS

A qualitative conceptual model of fault development places the Pirate fault in context relative to features observed along the fault and, in particular, accounts for major aspects of the fault exhibited at the Dead Hawk Gulch (DHG) reference site described below. It is taken as given that the fault is a down-to-the west, dip-slip, normal fault formed in response to sustained east-west Basin-Range extension that resulted in considerable (~4 km) vertical displacement on the fault. The resulting fault zone is considered to have developed by progressive linkage of subparallel fault segments (Gupta et al., 1998) to produce a central

fault core of indurated microbreccia and/or cataclasite a few tens of centimeters thick (Fig. 3) adjoined on hanging wall and footwall by damage zones composed of brecciated/fractured fault rocks extending a few tens of meters into the enclosing host rock (Chester et al., 1993). Cataclasis, accompanied by frictional heating as the hanging wall descended relative to the footwall, are considered to be the principal processes by which the fault-core rocks evolved.

common depth of fault emplacement. Accepting ~4 km as the vertical displacement on the fault and assuming isostasy and a land-surface denudation rate of ~0.3 mm/yr (inferred from Menges and McFadden (1981)), the depth of burial of the present-day exposed fault rocks likely was no more than ~4-6 km. Description of particular sites along the trace of the Pirate fault begins with discussion of the Dead Hawk Gulch (DHG) site, here considered to be a reference location of fault

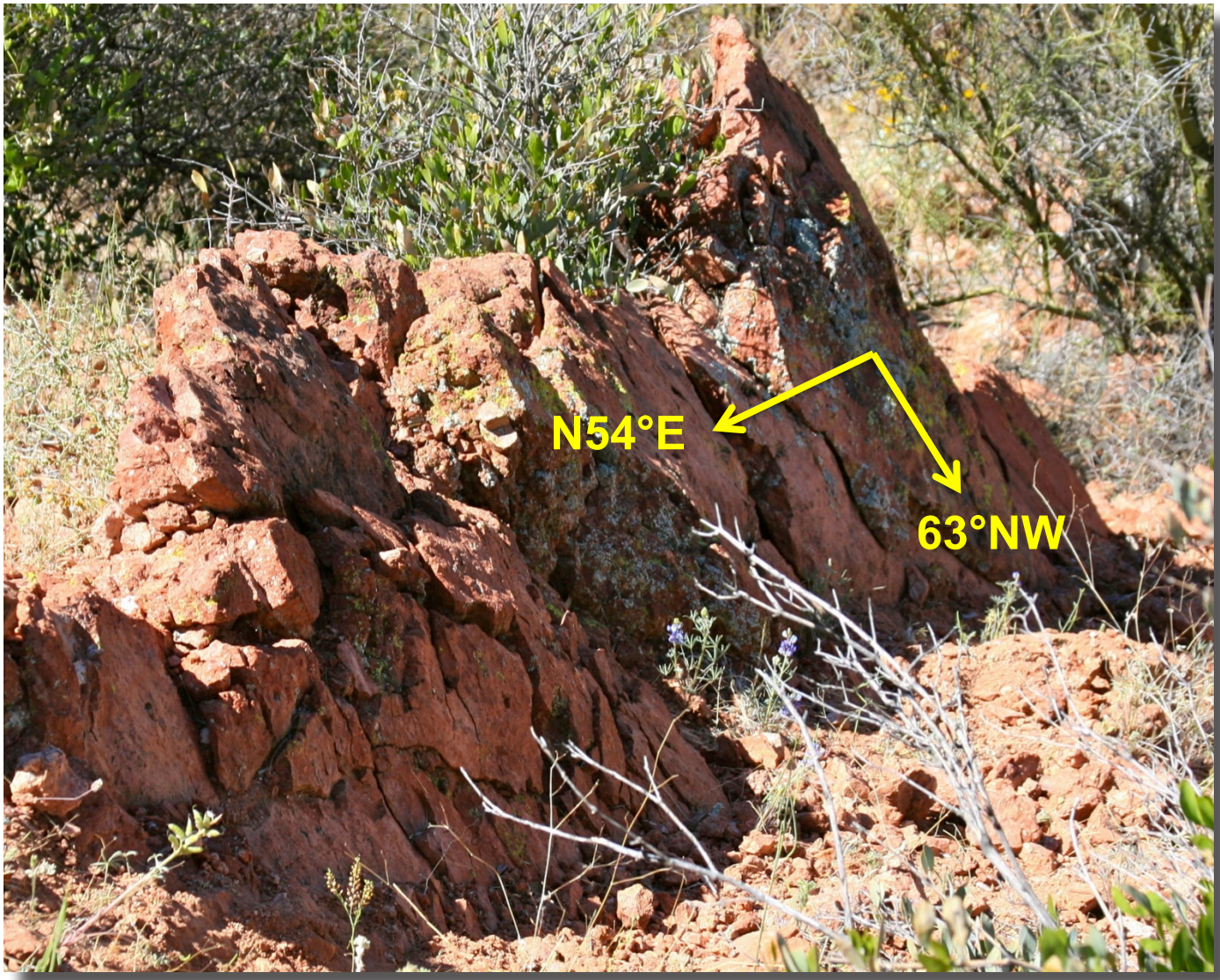

Figure 3. Oblique view of Pirate fault core cataclasite and fault surface, showing strike (N54°E) and dip (63°NW), exposed at the Alamo Canyon (ALC) site at (0508295 3585844).

PIRATE FAULT SITE DESCRIPTIONS

Altitude from north to south along the continuous trace of the Pirate fault depicted in Figs. 2A-E ranges from ~1050 m to ~900 m. Hence the ensemble of sites of exposed fault rocks constitutes a single ~150 m-thick horizon that, to good approximation, references a

morphology, followed by description of other sites from north to south along the trace of the fault. In most cases the sites are well accommodated by the adopted conceptual model but some sites exhibit discrepancies with respect to the conceptual model and/or the DHG reference site whose interpretations in some instances remain to be fully elucidated.

Dead Hawk Gulch (DHG) Site

The Pirate fault is well exposed at the DHG site (Fig. 2A) where its transect through Tgc host rock is expressed on the footwall as a ~200 m-thick fault zone divided, from top to bottom, into five structural units (Davis et al., 1998, 2004): (1) a convex-outward, smooth fault surface dipping ~50°W; (2) a thin (~10 cm) "compact breccia sheet" oriented parallel to the fault surface; (3) a thick middle zone (~180 m) of "cohesive" brecciated Tgc cut by fractures, shear surfaces, and cataclasite dikes; (4) a lower ~40 m-thick "fracture grid network" consisting of orthogonal fracture sets in unbrecciated Tgc locally intruded by cataclasite dikes; and (5) basal undeformed Tgc footwall bedrock. This structural representation accords well with the conceptual model adopted for this study in which Units 1 and 2 above constitute the fault core and Units 3 and 4 above make up the damage zone at this site. The "compact breccia sheet," Unit 2 above, commonly is not present at other sites where the fault surface is exposed but, rather, the fault core at these sites typically consists of a ~1 m-thick siliceous, usually red-matrix cataclasite on which the fault surface is impressed. Like many of the other sites where fault core rocks are exposed, conspicuous red hematite has pervaded the entire suite of fault-related rocks, fractures, and cataclasite dikes at the DHG site. In the absence of detailed chemical analyses or x-ray diffraction data, "hematite" here refers to any or all of the suite of ferric oxyhydroxides that may contribute to the ochre-colored matrix of fault-core microbreccias and/or cataclasites as well as that of damage-zone breccia, cataclasite dikes, and fracture-filling material.

Because the well-documented fault characteristics (Davis et al., 1998, 2004) at the DHG site accord well with the conceptual model adopted for this study (Gupta et al., 1998; Chester et al., 1993), the DHG site is taken here to be a reference, or "type," location with respect to which fault characteristics at other sites are compared. However, it is emphasized that no one site of exposed fault rocks can be taken as representative of the Pirate fault as a whole. The considerable variability of fault characteristics and morphology relative to the DHG site emerged as a principal finding of the present study. Some of the variability can be ascribed to mere differences in detail, e.g., the presence or absence of hematite at specific sites, or as anomalies, such as the apparent leucogranite block (described below) on the hanging wall of the fault at the Alamo Canyon (ALC) site (Fig. 2D). On the other hand, the Breccia Hill Complex (BHC) (Fig. 2D) in Tgw host rock and the set of mafic dikes that apparently delineate the fault trace where it passes through Tgc host rock (Figs. 2A-C), are manifestations of the Pirate fault that depart significantly from the reference fault morphology at the DHG site.

XP Wash (XP1 and XP2) Sites

The XP1 and XP2 sites (Fig. 2A) are located ~700 m north of the DHG site and are the northernmost sites of exposed Pirate fault surface (at XP2) and fault core rocks (at XP1). At these sites the fault transects Proterozoic Pinal schist (Xp) host rock (Table 2), which at these sites consists of mostly fractured, moderately deformed greywacke intruded by quartz stringers and pods. Except for the absence of an exposed fault surface, the complete fault zone is exposed at the XPW1 site where it has a total thickness of ~60 m divisible structurally from top to bottom into three units: (1) a ~30 cm thick indurated fine-grained fault core overlain by hanging-wall Qal and underlain by (2) a ~10 m-thick zone of pulverized Xp situated on top of (3) a ~50 m-thick damage zone of variably fractured and brecciated Xp. These units seem to correlate straightforwardly with Units 2, 3, and 4, respectively, at the DHG site. Hematite appears to be absent within the Xp fault-zone rocks while calcite is locally abundant as infilling material. At the XPW2 site, ~200 m north of XPW1, a small drainage has cut through Qal overburden to expose a planar fault surface, striking ~15° NW and dipping ~54° SW (Dickinson, 1994), expressed on underlying Xp host rock. Except for the difference in detail posed by the presence of calcite and the absence of hematite, the overall Pirate fault morphology presented by the combined XP1 and XP2 sites appears to accord well with that exhibited at the DHG reference site.

Golder Dam (GD) Site

The GD Site (Fig. 2A) is located in and adjacent to the floor of Cańada del Oro about 1.4 km south of the DHG site. The fault is expressed by a ~1 m thick, red-matrix cataclasite core and fault surface, striking ~N13°E and dipping ~57°W, situated ~5 m above the valley floor on the west side of the stream channel. The footwall consists of an ~80 m-thick, hematite-rich damage zone of variably fractured Tgc host rock. An

apparent anomaly is the presence of a ~10 cm-thick mafic dike intruded along the hanging-wall face of the fault-core cataclasite.

Mafic Dike (MFD) Sites

Apparently, beginning at the GD site mafic dikes intrude Tgcg fault breccia parallel and adjacent to the fault-rock/host-rock contact and appear to delineate the trace of the Pirate fault for at least ~10 km southward through Tgc host rocks (Figs. 2A-C). The dikes are especially well exposed in the interval from (0512573 3595710) to at least (0512480 3595404) (Fig. 2B), where a set of two or more parallel mafic dikes separated by intercalated Tgcg breccia and Tgc host rock are exposed for a mapped length of ~600 m. The dike set is ~40 m wide and each dike of the set displays a coarse-grained "gabbroic" core with aphanitic margins in direct contact with Tgcg breccia or Tgc host rock (Fig. 4). At (0512527 3595544), here designated the MFD site in Fig. 2B, the westernmost dike of the set exposes a smooth planar surface that strikes ~N10°E and dips ~55°W, essentially coincident with the strike of N13°E and dip of 50°W reported for the Pirate fault at this location (Dickinson, 1994). However, the reported Pirate fault attitude (Dickinson, 1994) makes no note of the presence or use of a mafic dike as a surrogate or delineator of the fault surface so it is not clear that these two measured attitudes refer either to the same feature or to the same site. Based on the evidence of apparent coincidence of the fault trace with intruded mafic rocks along this segment of the fault, it is accepted here that the orientation of the mafic dikes and the exposed smooth planar face at the MFD site are indirect but compelling indicators of the Pirate fault trace.

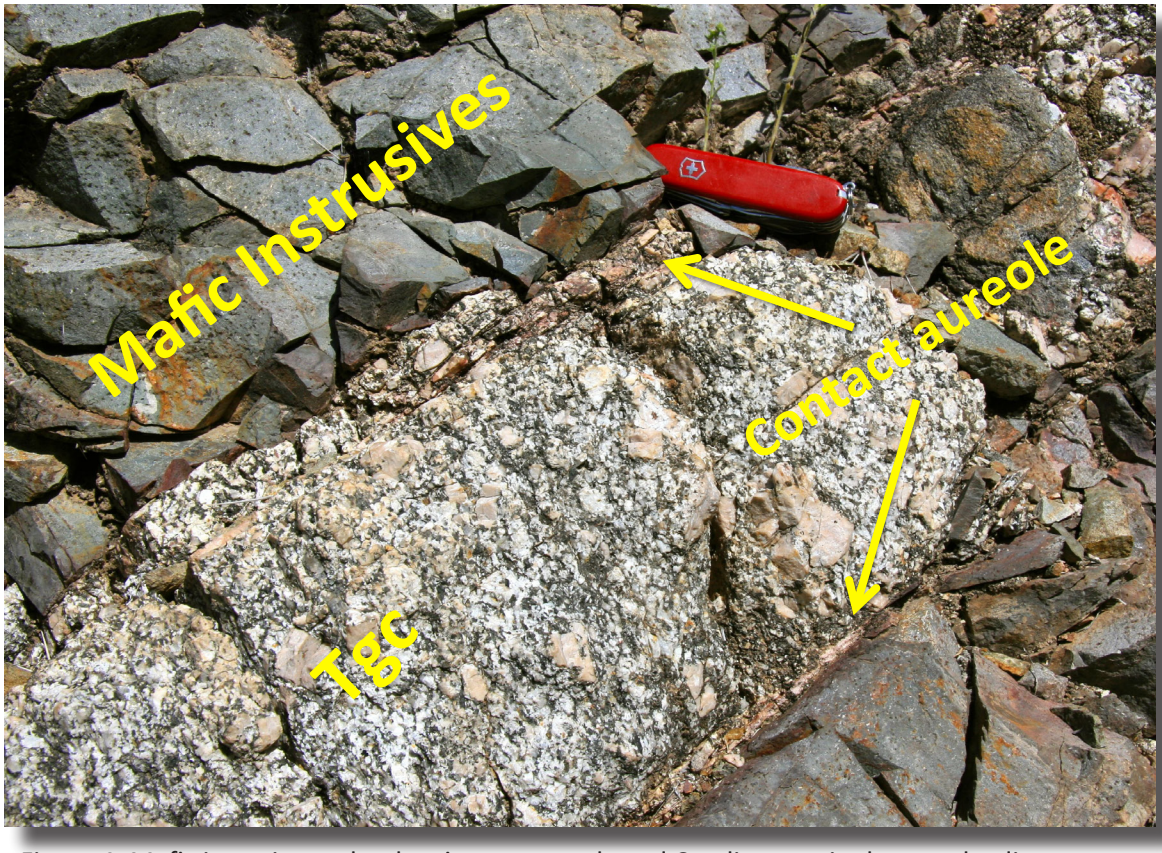

Figure 4. Mafic intrusive rocks abutting contact altered Catalina granite host rock adjacent to Pirate fault footwall at (0512549 3595647).

The occurrence of mafic dikes intruding Pirate fault rocks within Tgc host rock is not reported in the literature consulted during the present study. That fault zones serve as conduits for opportunistic injection of upwelling magma into pre-existing fault rocks is well known, e.g. (Gilbert and Reynolds, 1973), and such may apply to the mafic dikes associated with the Pirate fault as well. The mafic dikes of the Pirate fault intrude Tgcg hanging-wall breccia at and parallel to Tgcg contact with adjacent Tgc footwall bedrock. It thus seems clear that the dikes are related intimately to the presence

of the fault. The Tgcg breccia, however, appears to be free of mafic-rock fragments derived from the intruded mafic dikes, implying that the dikes were intruded after Tgcg had accumulated on the hanging wall during uplift of Tgc host rock. Hence, intrusion of the mafic dikes appears to be an event associated with the Pirate fault that occurred late in the active life of the fault. In the absence of petrologic analysis and age dates, however, the origin and timing of the mafic-rock intrusions and their possible relationship with the Pirate fault remain conjectural.

Romero-Cargodera (RCX) Site

The RCX site (Fig. 2D) is located about 6 km south of the MFD site (Fig. 2B) and is situated in a somewhat enigmatic setting in which, from south to north, the Pirate fault apparently jogs to the east and bends to the north (Fig. 2C). The jog and bend is interpreted by Dickinson (1994) to be a "bedrock ramp between master [Pirate] fault and [a] splay fault" and shows the splay fault as branching from the main Pirate fault near the mouth of Romero Canyon (Fig. 2D) and striking almost due north. As discussed below, however, the presence of a splay fault and bedrock ramp does not appear to accord with field evidence at the site. Nevertheless, the jog and bend effectively divides the Pirate fault into northern and southern segments in which the strike of the fault changes abruptly from ~N50°E in the south to ~N10°E in the north.

Geologic evidence at the RCX site consists of a window in Qal overburden that exposes poorly cohesive leucocratic-granite crush breccia at the RCX site location at (0510313 3588634) and extends ~150 m to the east as a zone of hematite-free, complexly brecciated/fractured leucocratic granite to its eastern contact with undeformed Tgw host rock at (0510462 3588638). The zone is interpreted here straightforwardly to express the Pirate fault footwall damage zone at this site, and, in this context, to represent the surface trace of the fault without introduction of a splay fault or a bedrock ramp. To account for the apparent jog and bend in the fault trace, Dickinson (1994) notes that the RCX site aligns approximately with a northwesterly continuation of the Romero Pass fault zone (Fig. 1) that strikes ~N55°W across the central Santa Catalina Mountains structural block (Force, 1997) and suggests that plausible residual presence, as depicted in Fig. 2D, of the Romero Pass fault zone may have influenced formation of the Pirate fault at the RCX site. Dickinson (1994) acknowledges, however, that there is no firm evidence for passage of the Romero Pass fault across the western Santa Catalina mountain front. It should be noted, perhaps, that the RCX site is located virtually at the contact between Mid-Miocene Tgc host rock to the north and Eocene Tgw host rock to the south. Hence, discontinuity of rock properties at and across the boundary between adjoined Tgc and Tgw host rocks is considered here, possibly, to have influenced both morphology and direction of the Late-Miocene Pirate fault and, thereby, to have contributed to formation of the apparent jog and bend in fault orientation at this location.

Breccia Hill Complex (BHC)

The BHC (Fig. 2D) is demarcated by two prominent, fault-related, topographic features, informally named "Breccia Hill North" (BHN) at (0510316 3588249) and "Breccia Hill South" (BHS) at (0510035 3587765). These features are connected from north to south along the trace of the Pirate fault by an ~80 m-thick, ~545 m-long damage zone of brecciated/fractured Tgw host rock. Neither fault-core rocks nor a fault surface is exposed at the BHC but either or both of these may be present beneath the Qal that abuts and overlies the BHC on the west (Spencer and Pearthree, 2004). Both BHN and BHS are outcrops of indurated fault breccia composed of lichen-encrusted, cobble-sized quartz/feldspar blocks imbedded in a cohesive groundmass of pea-to-pebble-sized Tgw breccia. The fragmented groundmass locally forms breccia dikes and sills but for the most part the orientations of the breccia fragments appear to be random. The dominant mineral assemblage consists of white-to-tan feldspar with gray quartz and minor dark minerals. Whether noteworthy or not, hematite appears to be largely absent at this site.

The damage zone exposed between BHN and BHS is well displayed at the south end of the BHC, where it structurally underlies BHS. The ~80 m-thick zone consists of upper, poorly cohesive breccia of mostly ≤1-2 cm white feldspar clasts that grades into lower fractured Tgw host rock overlying footwall bedrock. This structural setting of a breccia zone overlying a "fracture grid network" that, in turn, overlies undeformed host rock seemingly correlates with Units 3 and 4 at the DHG site and, if so, possibly is the only fault characteristic common to both the BHC and DHG

sites. Contact between this fracture grid network and underlying Tgw host rock at BHS is along a planar shear surface that strikes ~N10°W, dips ~45°S, and is traceable from (0150143 3587797) in the southeast to at least (0510112 3587936), ~150 m to the northwest. The shear fracture is one of a set of parallel, closely spaced (~10 m), southeast-northwest trending shear joints cutting Tgw host rock at this location.

The conditions and dynamics that produced the Pirate fault-related features at the BHC remain to be fully explicated. Dickinson (1994) notes that, like the RCX site discussed above, the BHC also is aligned approximately with the projected northwestward continuation of the Romero Pass fault zone (Fig. 1) Here it is suggested that mutually oblique intersection (in both strike and dip) of the Pirate fault with the host-rock shear joints described above together with a possible influence from relict Romero Pass fault zone could have produced a structural setting at the BHC that may have led to rather complex fault dynamics. For example, Spencer and Pearthree (2004) suggest that the cohesive Tgw breccia of BHN and BHS may have formed as "co-seismic implosion breccia" into "dilational voids" produced by seismic events on the Pirate fault. Whether such dynamics took place at the BHC remains to be determined, but what appears to be evident is that formation of the BHC entailed conditions and events significantly discordant with respect to the simple conceptual model of Pirate fault formation adopted here as exemplified by the DHG reference site.

Pirate Knob (PK) Site

At the Pirate Knob (PK) site (Fig. 2D), approximately 2.5 km southwest of the BHC, well-exposed Pirate fault transects Kga host rock and displays fault characteristics that, in the main, accord well with those exhibited at the DHG reference site. The site features an exposed smooth, planar fault surface; a ~1 m-thick, red-matrix, "vesicular" fault-core cataclasite; and a ~50 m-thick damage zone consisting of poorly cohesive, hematite-rich Kga breccia abutting a vertical footwall scarp of Kga host rock. The vesicular fault-core cataclasite is confined largely to a ~10 cm-thick zone directly beneath the fault surface and appears to correlate structurally with the "compact breccia sheet," Unit 2 at the DHG site. The "vesicules" are ovoid cavities that range in diameter from ~1 mm to ~5 cm and appear to be the result of removal of material imbedded in the cataclasite. Similar cavities occur sparsely in exposed fault-core rocks at other sites but at this site the cavities greatly outnumber the ≤1 cm feldspar clasts imbedded in the fine-grained cataclasite matrix. Interiors of some of the cavities are coated with black manganese but otherwise there is no evidence of whatever material, if any, may have once filled these cavities. The vesicles are anomalous relative to the DHG and other sites of exposed fault-core cataclasite and their presence and origin at the PK site awaits further explication.

Alamo Canyon (ALC) Site

The ALC site (Fig. 2D) provides the best representative example of Pirate fault-zone characteristics along the southern trace of the fault. The fault is well exposed in the north wall of Alamo Canyon, which at this site is a ~30 m-deep gorge cut consecutively, from upstream to downstream, through Kga host rock, Pirate fault zone, and overlying Qal. The site reveals a footwall structural domain consisting, from top to bottom, of (1) a smooth, planar, manganese-coated fault surface impressed on (2) a ~1 m-thick fault core of red-matrix cataclasite (Fig. 3) underlain by (3) a ≥45 m-thick damage zone of hematite-rich host-rock breccia. Within the damage zone, brecciation decreases progressively with increasing structural depth while abundance of hematite-filled, through-going fractures increases in a manner correlative with Units 3 and 4 at the DHG site. Hence, the overall characteristics of the Pirate fault at the ALC site largely reproduce those at the DHG site except, however, for a complication.

Because of its burial beneath debris eroded from the Santa Catalina structural block following cessation of active uplift, the Pirate fault, where exposed, nominally abuts Qal residuum on the hanging wall. At the ALC site, however, the Pirate fault is in direct contact on the hanging wall with a block of hematite-free leucogranite. Although partly covered by hill-slope debris, the block is traceable for at least ~400 m to the northwest, perpendicular to the N54°E strike of the fault surface at the site. The full three-dimensional configuration of the block could not be determined; however, outcrops of leucogranite at many locations between the distal point at (0508023 3586167) and contact of the block with the Pirate fault surface at (0508295 3585844) indicate the block to be a shattered but otherwise intact entity. Although the block is highly

fractured neither shear surfaces nor slickensides were observed at any of the leucogranite outcrops examined during this study. Between (0508248 3586063) and its terminal point at (0508023 3586167), the block forms the crest of a ridge between Alamo Canyon to the south and a small drainage to the north incised at the contact between the block and overlying Qal. At the (0508023 3586167) terminal point the drainage cuts through the ridge beyond which point the block, if present, is covered by Qal. No outcrops of the block were observed on the Qal-covered south wall of Alamo Canyon.

At its contact with the red-matrix fault surface, the leucogranite is highly brecciated (Fig. 5) for a distance of ~25 m normal to the fault surface suggesting that mechanical grinding and pulverization were the principal agents that produced the breccia. The leucogranite is composed almost entirely of hematite-free, white feldspar with light-gray-to-clear quartz inclusions and only minor abundance of dark minerals; however, it locally encloses pods and seams of biotite-rich granite. The presence of garnet in the leucogranite suggests it to be Tgw, which both intrudes and overlies Kga host rock at this location (Spencer and Pearthree, 2004). The biotite-rich granitic seams and pods observed at some of the nominally leucogranite outcrops thus may be Kga inclusions in otherwise Tgw host rock.

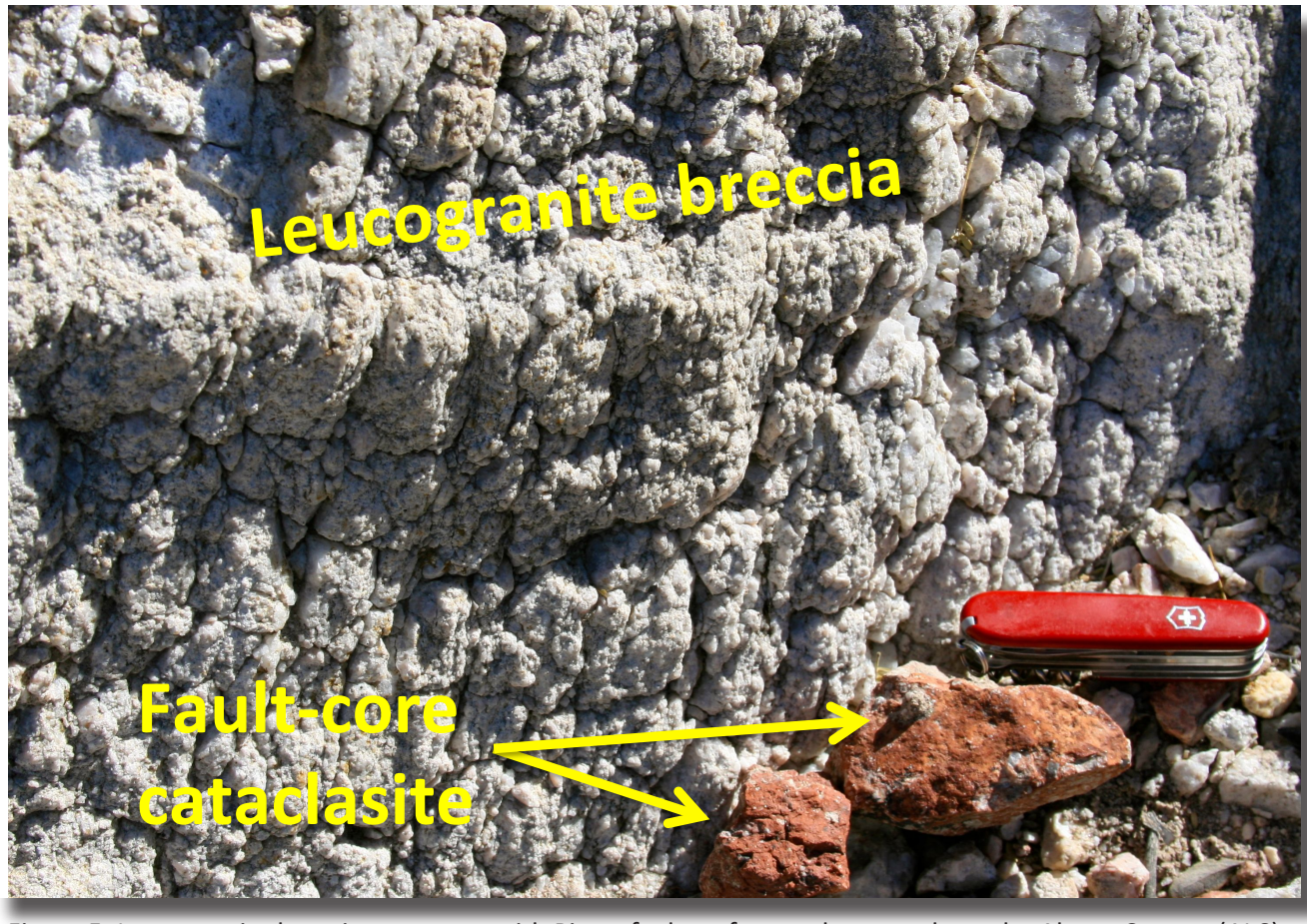

Figure 5. Leucogranite breccia at contact with Pirate fault surface and core rocks at the Alamo Canyon (ALC) site at (0508295 3585844). Hematite-rich fault-core cataclasite samples shown for contrast/comparison at base of photo.

That the block is hematite-free while the adjoining fault-core cataclasite and footwall damage zone are hematite-rich seemingly implies the block to have been emplaced after hematite was deposited in the Pirate fault at this site. Hence the block gives the appearance of having been sundered from an upper section of hanging-wall damage-zone and lodged in its present-day configuration during active uplift on the fault. Although the leucogranite outcrops are sufficiently numerous to establish the presence and some properties of the block on the nominal hanging wall of the fault, they do not allow determination of either the full extent of the feature or its spatial configuration.

Perhaps the block is a subsidiary imbricate fault block structurally associated with the presumed listric nature of the Pirate fault (cf. Wernicke and Axen 1988, Fig. 4c) or perhaps it is an isolated "sidewall ripout" rent from the hanging wall by local splaying or bifurcation of the fault in the manner described by Swanson (2005). A seemingly less likely alternative may be that the block is a landslide block of footwall host rock that fortuitously managed to slide down more-or-less intact along the fault surface to lodge in its present-day location.

Pusch Ridge Wilderness (PRW) Site

The Pusch Ridge Wilderness (PRW) site (Fig. 2D), ~0.8 km southwest of the ALC site, features a 185 m-long by ~1 m-thick hematite-rich fault-core cataclasite "dike" abutted by Qal on the hanging-wall and by a ~50 m-thick damage zone of poorly exposed Kga host-rock breccia on the footwall. The fault-core cataclasite is composed of ≤2 cm feldspar clasts imbedded in well-indurated siliceous, hematite-rich matrix and exposes a smooth planar fault surface striking N55°E and dipping 54°NW, typical of the southern segment of Pirate fault. The PRW site is notable for being the only site visited that did not appear to exhibit some difference or anomaly with respect to the DHG reference site

Linda Vista Trail (LVT) Site

The Linda Vista Trail (LVT) site (Fig. 2E) is the southernmost of the known accessible exposures of Pirate fault-core rocks. The fault is expressed here as a ~30 m-thick by ~30 m-long zone of Kga fault breccia whose centerpiece is a ~3 m-thick fault core composed of up to pebble-sized quartz/feldspar clasts imbedded in a reddish-brown, fine-grained, hard, siliceous matrix. Most of the fault zone at this site is covered by surficial debris, which prevented detailed examination of fault morphology and of the contacts of the fault with hanging-wall Qal and footwall Kga host rock. Given the incomplete exposure of the fault zone at this site, only the presence of the fault is firmly established and little can be ascertained of overall fault morphology. Similar assessment applies to the three unlabeled sites shown by filled triangles in Figs. 2D-E, where fault-core rocks are exposed but with incomplete exposure of the entire fault zone. The relatively thick (~3 m) fault core exposed at the LVT site together with the relatively large clasts (up to ~6 cm) imbedded in the fault core rocks, however, are considered anomalous relative to the DHG reference site.

GEOLOGY OF THE INFORMAL Tgcg STRATIGRAPHIC UNIT

The informally defined and, apparently, previously unrecognized Tgcg unit (Table 2) is here introduced as an outcome of the present study. The unit is composed almost entirely of accumulated Tgc detritus with little, if any, contribution from other sources and is exposed continuously for ~ 5 km from (0513575 3600207) in the north to at least (0512435 3595285) in the south (Figs. 2A-B). The unit essentially constitutes the hanging wall of the Pirate fault where the fault transects Tgc host rock. The unit's eastern extent is marked by Tgcg breccia in direct contact with Tgc host rock and locally intruded by mafic dikes. The western boundary of the unit is formed by the Cañada del Oro, which cuts through ~20-m-thick, light-colored Tgcg overlain by ~3 m-thick cobble/boulder Qal to form steep valley sides along the active stream channel. These valley-side "scarps" beneath overlying Qal are composed of fine-grained, cohesive, stratified, but poorly graded and sorted Tgcg with occasional embedded granitic (presumed Tgc) pebbles, cobbles, and boulders (Fig. 6). Indurated Tgcg forms the "bedrock" floor of the Cañada del Oro drainage for a distance of ~750 m from north to south between (0513580 3599960) and (0513432 3599201) and is mapped as "Tgcg" in Figs. 2A-B. Although these Tgcg outcrops are not fault rocks per se, they are significant artifacts of the Pirate fault that appear to record a period of rapid, perhaps aseismic, uplift that kept pace with equally rapid disintegration of Tgc host rock along that segment of the fault through Tgc bedrock. That the Tgc erodes relatively easily is evident from the rapid weathering of present-day outcrops and implied by noting that the post-Pirate fault pediment formed along the western Santa Catalina mountain front attains its maximum width of ~4 km along that interval where the fault transects Tgc host rock.

DISCONTINUOUS DISTRIBUTION OF HEMATITE ALONG THE FAULT

With apparent exception of the RCX, MFD, and BHC sites most of the variability in fault characteristics along the Pirate fault can be accommodated within the framework of the adopted conceptual model

as exemplified by the fault morphology at the DHG site. An anomaly that may have no direct bearing on the conceptual model concerns the discontinuous distribution of hematite along the Pirate fault. Hematite, regarded here to comprise any or all of whatever ferric oxyhydroxides may be present, appears to be common as red matrix material and gouge in faults in the granitic terrains of the Santa Catalina Mountains (Force, 1997). The Sabino Canyon fault in the southern Santa Catalina Mountains (Fig. 1) provides an easily accessible example. The Sabino Canyon fault (Force, 1997; Bezy, 2004) is a down-to-the east, north-south trending, dip-slip, normal fault that transects metamorphosed and undeformed granitoid rocks from the mouth of Sabino Canyon at the south to intersection of the fault with the Romero Pass fault zone ~7 km to the north (Fig. 1). The fault trace is readily accessible by foot and shuttle bus at a number of locations in the lower reaches of Sabino Canyon (Bezy, 2004). Where exposed, e.g., in road cuts midway between the Sabino Canyon Visitor's Center and Shuttle Stop 1 and between Shuttle Stops 8 and 9, the fault is expressed as a ~1 m-thick zone composed of locally slickensided, red-matrix breccia and gouge (Bezy, 2004). A signature distinction between the Sabino Canyon and Pirate faults, however, is that hematite appears to be distributed continuously along the trace of the Sabino Canyon fault but is distributed discontinuously along the trace of the Pirate fault.

Direct deposition of ferric oxyhydroxides from percolating groundwater seems an unlikely source of the hematite observed in the Sabino Canyon and Pirate faults. Deposition of ferrous iron from cooling hydrothermal solutions rising into and along the fault damage zone followed by subsequent oxidation by descending, oxygen-rich meteoric water would seem to be the more likely geochemical process involved. Hot groundwater, upwelling along or associated with mountain-front normal faults, is characteristic of the present-day, tectonically active parts of the Basin and Range Province (Eaton, 1982) and, by extrapolation, likely occurred during the active Basin-Range disturbance that produced the Pirate fault. Spencer and Pearthree (2004) suggest hydrothermal upwelling and deposition to be the source of hematite where present in the Pirate fault zone. However, there are several sites along the Pirate fault where hematite is absent, and this discontinuous distribution of fault-related

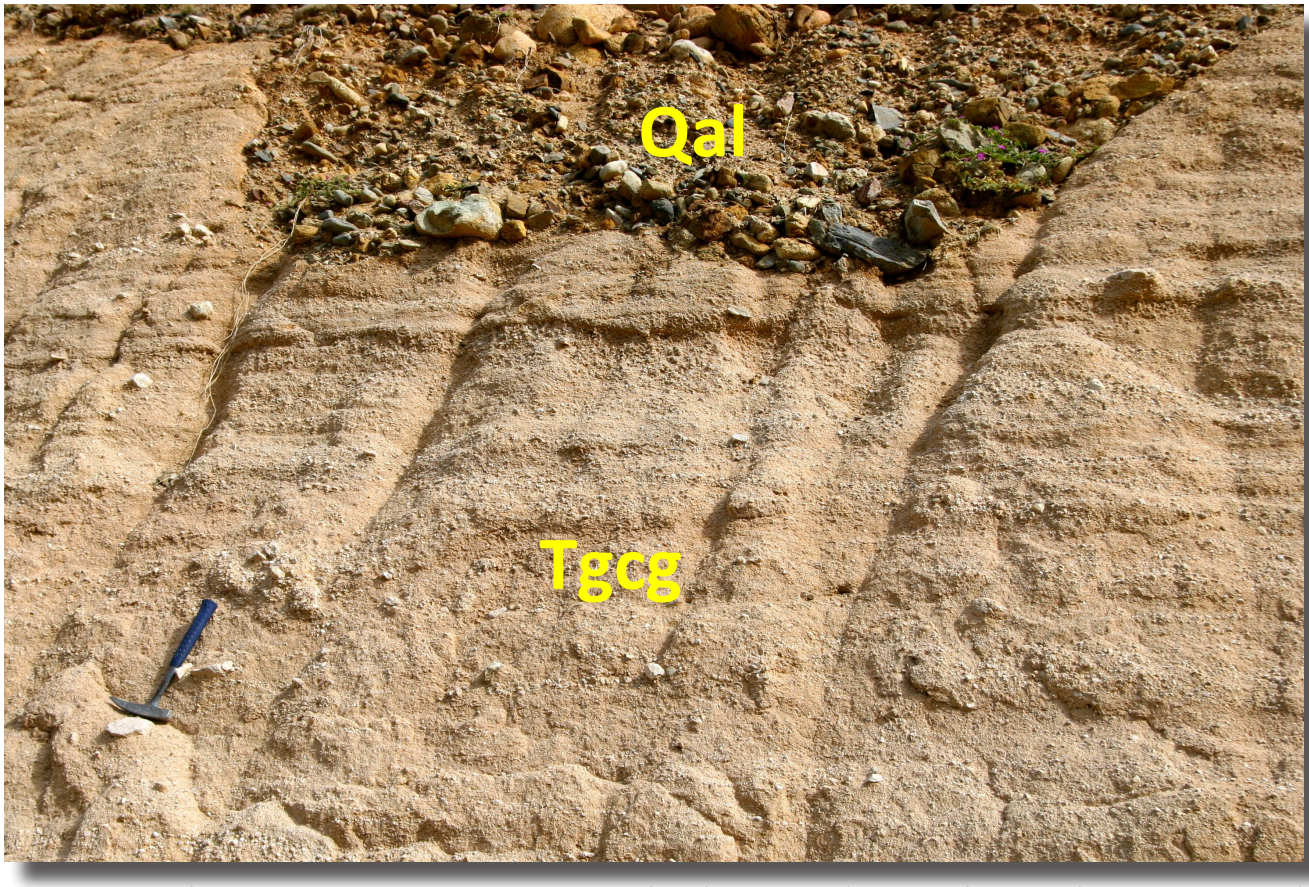

Figure 6. Stratified Tgcg unit overlain by Cordones surface (Pleistocene) cut-and-fill Qal at (0513438 3600125).

hematite raises questions about what hydrothermal environments may have prevailed at depth within the fault zone. It may be argued that hematite deposition was localized and thereby restricted to specific locations along the fault. It is difficult, however, to reconcile this with the perhaps naïve but seemingly plausible notion that hydrothermal fluids upwelling within the Pirate fault not only would tend to seek a common hydrostatic level but also would tend to pervade the entire trace of the fault laterally to whatever be that common level. Such circumstance would seem to explain the apparent continuous distribution of hematite along the Sabino Canyon fault from a low-point altitude of ~850 m near the mouth of Sabino Canyon to at least an altitude of ~1000 m between Shuttle Stops 8 and 9.

The northernmost site along the Pirate fault with conspicuous hematite is the DHG site (Fig. 2A) at an altitude of ~1000 m while the southernmost is the LVT site (Fig. 2E) at an altitude of ~900 m. These two sites are separated laterally by a distance of ~20 km along the fault and differ in altitude by ~100 m. The BHC (Fig. 2D), at which hematite is conspicuously absent, is located ~10.5 km south of the DHG site at an altitude of ~885 m. Hence the BHC is situated approximately midway between the DHG and LVT sites, but with an altitude ~115 m below that of the DHG site and ~15 m below that of the LVT site. If hematite were to have been deposited along the fault to at least the altitude of the DHG site, it follows that hematite would be expected at the LVT site, as observed, but also should have been deposited at the BHC. Perhaps, indeed, hematite was deposited at the BHC but, following deposition, oxygen-depleted groundwater entered the fault locally to create reducing conditions that converted insoluble ferric iron to soluble ferrous iron that subsequently was removed by the descending groundwater. A problem with this scenario, however, is that water descending along the fault most likely would be oxygen-rich meteoric water that would not become sufficiently oxygen depleted on passage through granitic fault-zone rocks to create reducing conditions. Alternatively, Jang et al. (2007) report that prolonged hydration of hematite converts the exposed outer surface of hematite to more soluble goethite and/or hydrous ferric oxide so that over time in the presence of sufficient water it would seem conceivable that hematite could be removed locally from a site such as the BHC. Nevertheless, these arguments seemingly lead to choosing between a Charybdis of localized hematite deposition and a Scylla of localized hematite removal to account for the observed discontinuous distribution of hematite along the Pirate fault.

Some clues to the origin of hematite in the Pirate fault zone are offered by the anomalous appearance at the ALC site of the hematite-free, hanging-wall leucogranite block described above. That the block is in direct contact with exposed fault surface and hematite-rich fault-core cataclasite implies hematite deposition to have been confined both to a discrete time interval that ended before emplacement of the hematite-free leucogranite block and to a vertical interval whose upper boundary lay below that of the displaced leucogranite block. Another observation is that at all sites of hematite-rich fault-core rocks, hematitic material is distributed uniformly throughout the matrices of both the microbreccia/cataclasite fault core and the underlying damage zone suggesting that hematite was present during fault-core cataclasis. The implication may be that hematite deposition, by whatever means, was integral to and occurred early during Pirate fault formation and was followed by the Syclla of localized removal at specific locations by processes as yet unidentified.

SUMMARY AND CONCLUSION

Field examination of exposed fault rocks and fault-related features along the exhumed trace of the Pirate fault was undertaken to assemble as complete a suite of surface evidence as possible by which to identify, describe, and interpret the processes and events that produced the fault in its present-day configuration. What emerges from this study is that the Pirate fault, considered in its entirety, comprises more than is revealed at any one site. While the main trace of the fault accords well with a relatively simple conceptual model of fault development, a number of sites along the fault exhibit site-specific disparities or anomalies, the elucidation of whose characteristics became a major focus of this study. Some of these disparities and anomalies possibly can be interpreted in terms of features reported in studies of other faults, e.g., the fault-zone mafic intrusions and the occurrence of a seemingly anomalous hematite-free hanging-wall block abutting hematite-rich fault-core footwall, but others, such as the discontinuous distribution of hematite along the fault, would seem to defy ready explanation. The picture that emerges is that of the Pirate fault as

a geologic entity whose tenure as an active participant in the extensional Basin-Range tectonic event has left behind a somewhat sparse and locally enigmatic set of remains from which to infer, caveat emptor, its past.

ACKNOWLEDGEMENTS

The author expresses his gratitude to colleagues Arend Meijer for helpful comments on an early draft of the manuscript and Brian Holtslag for field assistance.

REFERENCES CITED

Bezy, J.V., 2004, A guide to the geology of Sabino Canyon and the Catalina Highway, Coronado National Forest: Arizona Geological Survey, Down-to-Earth 17, 45 p.

Chester, F.M, Evans, J.P., and Biegel, R.L., 1993, Internal structure and weakening mechanism of the San Andreas fault: Journal of Geophysical Research, v. 98, p. 771-786.

Davis, G.H., Bedford, J.M., Constenius, K.N., Johnson, J.A., Kong, F., Ornelas, R., Pecha, M., and Rodriguez, E.P. 1994, Deep cataclastic counterparts of neotectonic fault-rock architecture in the granite footwall of the Basin and Range Pirate fault, southern Arizona: Geological Society of America Abstracts with Programs, v. 26, no. 7, p. A267-A268.

Davis, G.H., Rodriguez, E.P., Cox, L.J., Ornelas, R., Constenius, K.N., Johnson, J.A., Kong, F., Bedford, J.M., and Pecha, M., 1998, Cohesive crush breccias, microbreccias, and cataclasites in granitic footwall of a normal fault, in Snoke, A.W., Tullis, J.A., and Todd, V.R., eds., Fault-related rocks: A photographic atlas: Princeton, New Jersey, Princeton University Press, p. 160-163.

Davis, G.H., Constenius, K.N., Dickinson, W.R., Rodriguez, E.P., and Cox, L.J., 2004, Fault and fault-rock characteristics associated with Cenozoic extension and core-complex evolution in the Catalina-Rincon region, southeastern Arizona: Geological Society of America Bulletin, v. 116, p. 128-141.

Dickinson, W.R., 1992, Geologic map of Catalina core complex and San Pedro trough, Pima, Pinal, Graham, and Cochise Counties, Arizona: Arizona Geological Survey Contributed Map CM-92-C, 1 sheet.

Dickinson, W.R., 1994, Trace of main displacement surface (bedrock/basin-fill contact) of Pirate fault zone, west flank of Santa Catalina Mountains, Pima and Pinal Counties, Arizona: Arizona Geological Survey Contributed Map CM-94-G, scale 1:24,000, I sheet, with 9 p. text.

Dickinson, W.R., 1999, Geologic framework of the Catalina foothills, outskirts of Tucson (Pima County, Arizona): Arizona Geological Survey Contributed Map CM-99-B, scale 1:24,000, 1 sheet, with 31 p. text.

Eaton, G.P., 1982, The Basin and Range Province: Origin and tectonic significance: Annual Review of Earth and Planetary Sciences, v. 10, p. 409-440.

Fenneman, N.M., 1931, Physiography of Western United States: New York and London, McGraw-Hill Book Co., 534 p.

Force, E.R., 1997, Geology and mineral resources of the Santa Catalina Mountains, southeastern Arizona: A cross-sectional approach: Tucson, University of Arizona Center for Mineral Resources Monographs in Mineral Resource Science 1, 135 p.

Gilbert, C.M. and Reynolds, M.W., 1973, Character and chronology of basin development, western margin of the Basin and Range Province: Geological Society of America Bulletin, v. 84, p. 2489-2510.

Gupta, S., Cowie, P.A., Dawers, N.H., and Underhill, J.R., 1998, A mechanism to explain rift-basin subsidence and stratigraphic patterns through fault-array evolution: Geology, v. 26, p. 595-598.

Jang, J-H, Dempsey, B.A., and Burgos, W.D., 2007, Solubility of hematite revisited: Effects of hydration: Environmental Science and Technology, v. 41, 7303-7308.

Menges, C.M., and McFadden, L.D., 1981, Evidence for a latest Miocene to Pliocene transition from basin-range tectonic to post-tectonic landscape evolution in southeastern Arizona: Arizona Geological Society Digest, v. 13, p. 151-160.

Spencer, J.E., and Pearthree, P.A., 2004, Geologic map of the Oro Valley 7½' Quadrangle and the Pusch Peak area, northeastern Pima County, Arizona: Arizona Geological Survey Digital Geologic Map 21, version 2.0, 1 sheet.

Swanson, M.T., 1989, Sidewall ripouts in strike-slip faults: Journal of Structural Geology, v. 11, p. 933-948.

Wallace, R.M., 1954, Structures at the northern end of the Santa Catalina Mountains, Arizona [M.S. Thesis]: Tucson, University of Arizona, 45 p.

Wernicke, B., and Axen, G.J., 1988, On the role of isostasy in the evolution of normal fault systems: Geology, v. 16, p. 848-851.